THE JOURNAL OF PHYSICAL CHEMISTRY B

Article

pubs.acs.org/JPCB

Effects of Interaction of Ionic and Nonionic Surfactants on Self-Assembly of PEO–PPO–PEO Triblock Copolymer in Aqueous Solution

J. S. Nambam and John Philip*

SMARTS, NDED, Metallurgy and Materials Group, Indira Gandhi Centre for Atomic Research, Kalpakkam 603 102, Tamilnadu, India

ABSTRACT: We study the effects of interaction of surfactants on the self-assembly of a triblock copolymer in aqueous solution by measuring percolation transition temperature (T_p), micellar size, zeta potential, and rheological properties. We use PEO–PPO–PEO triblock copolymer (Pluronics-F108) with anionic sodium dodecyl sulfate (SDS), cationic cetyltrimethylammonium bromide (CTAB), and nonionic nonylphenolethoxylate (NP9) for our investigations. The addition of SDS in pluronics solution leads to a dramatic reduction in the viscoelastic properties, while it remains almost unaffected with CTAB and NP9. The 2 orders of magnitude decrease in the elastic modulus in the presence of SDS indicates a soft solid-like microstructure formed by aggregating self-assembled triblock polymers. Our results indicate a strong electrostatic barrier imparted by the headgroup of SDS at the core–corona interface that inhibits the formation of hexagonally packed layers of micelles and the packing order. The analysis of autocorrelation function at high concentrations of ionic surfactant indicates that pure surfactant micelles coexist with large intermicellar structures. With increasing surfactant concentration, the zeta potential of the pluronic micelle is found to decrease. These results suggest that the microstructure and elastic properties of block copolymer micelles can be tuned by varying the concentrations of ionic surfactant that enhances their potential in applications as nanocarriers for drug delivery systems.

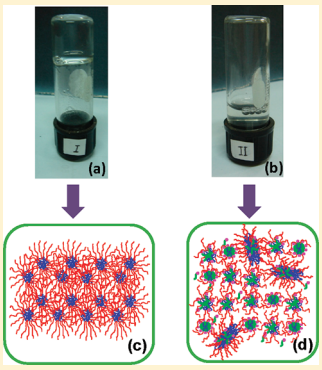

1. INTRODUCTION

Triblock copolymers have been a topic of intense research for the last few decades due to their widespread applications in detergency, emulsification, drug delivery systems, gels for replacing biological fluids, and synthesis of different nanostructures.[1−9] Phase behaviors,[10−36] aggregation,[30,37] self-assembly,[38−42] rheological properties,[43−48] structure of micelles, and the interaction of triblock copolymers with surfactants[12,17,35,41,49−58] and nanoparticles[59] are systematically studied in the past. Besides, they are wonderful model systems to probe the competitive interaction between the constituting blocks and solvents leading to interesting metastable or stable mesoscopic structures[38,39,45,49,60,61] and for synthesis of biocompatible nanoparticles.[62] Recently, supermolecular formations of self-assembling triblock copolymers are elegantly demonstrated using nuclear magnetic resonance (NMR) diffusometry, which enabled probing structural and dynamic features of self-aggregation.[40] There are a few lucid reviews on block polymers too.[2,63] It is well established that poly(ethylene oxide)–poly(propylene oxide)–poly(ethylene oxide), denoted by PEO_m–PPO_n–PEO_m, commonly known as pluronic, form core–shell like micelles in aqueous solution, above a critical micelle concentration (CMC) or critical micelle temperature (CMT)[3] where the hydrophobic core is formed by propylene oxide (PO) groups and the hydrophilic corona region is formed by ethylene oxide (EO) groups. The self-aggregation arises from the limited temperature dependent solubility of the PPO block that gives rise to aggregates with a hydrophobic core surrounded by more hydrophilic and hydrated PEO blocks.[26,64] At low pluronic concentrations, and above CMC, spherical micelles grow progressively to form polymer-like micelles (or worm micelles) as temperature increases. Such transitions were reported in aqueous solutions of Pluronic P85[30,32] and P84.[23,65−67] Unlike the swollen network of covalently cross-linked polymer chains of most traditional polymer gels, triblock copolymer gel is held together by reversible entanglements between coronae of neighboring micelles, due to the absence of covalent cross-linking between the micelles.[68]

The self-assembly of triblock polymers in water is well documented.[3,18,28,29,33−35,69−74] At low temperature, both PEO and PPO blocks are hydrophilic, hence soluble in water, and form a transparent solution. Here, the triblock copolymers remain as unimers surrounded by water molecules with hydrogen bonds formed between them. At higher temperatures (above CMC or CMT), molecular aggregation of hydrophobic PPO blocks leads to the formation of micelles. These micelles will have a hydrophobic PPO core and hydrophilic PEO shell.[70,75,76] The micellization of PEO_m–PPO_n–PEO_m copolymers in water is an endothermic process, driven by a decrease in the polarity of ethylene oxide (EO) and propylene oxide (PO) segments at higher temperatures.[77] Depending on the PEO/PPO ratio, these micelles exhibit a shape transition, at

Received: September 15, 2011
Revised: December 21, 2011
Published: January 4, 2012

elevated temperature, from spherical to rod-like or worm-like micelles.[20,23,32,33,66,78] The increase in the hydrophobicity of both PEO and PPO segments at higher temperature leads to a packing of more PPO segments in the core. Further, the expulsion of water from the core and the shrinking of PEO segments leads to a reduction in the interfacial curvature and the interfacial energy. This increase in hydrophobicity leads to a progressive transformation of micelles into cubic, hexagonal, and lamellar structures.[79] During the transformation, the core size decreases, and a Gaussian coil will have the smallest size when micelles assume the shape of a disk.[79]

Surfactants are often added to polymer solutions to alter the rheological properties and to enhance the stability of dispersions.[80] Such polymer−surfactant combination is being utilized in a wide range of applications.[1,81] The association mechanism and the break-up of the PEO_m−PPO_n−PEO_m micelles due to addition of ionic surfactants have been studied by calorimetry and scattering techniques,[17,82,83] cyclic voltametry,[54] time-resolved fluorescence, SANS,[84] and NMR.[85] The interaction between pluronics and nonionic surfactants was investigated by means of differential scanning and isothermal calorimetry,[54] static and dynamic light scattering,[53] and shear viscosity method.[52] Recently, Vieira et al.[12] studied micellization and adsorption of triblock copolymer $PEO_{23}PPO_{52}PEO_{23}$ with SDS, dodecyltrimethylammonium bromide (DTAB), and tetraethylene glycol monooctyl ether (C_8EO_4) using neutron reflectivity and surface tension where a synergistic interaction between polymer and ionic surfactants and a strong repulsive interaction with C_8EO_4 is observed. Newby et al. systematically studied the structure and flow behavior of binary mixtures of pluronic block copolymers by small-angle scattering, rheometry, and mobility tests.[48] Couderc et al.[86] observed a synergistic interaction in binary mixtures of the nonionic surfactant hexaethylene glycol mono-*n*-dodecyl ether ($C_{12}EO_6$) and pluronics F127. The questions we try to address from this study are the following: what is the effect of surfactant association with pluronics F108 on the percolating transition temperature (T_p) under shear, where the pluronics micelles form a permanent spanning structure? How do we reversibly and continuously tune the rheological properties and T_p of triblock polymers? In this study, we investigate the interaction of anionic (SDS), cationic (CTAB), and nonionic (NP9) surfactants with the triblock copolymer F108. We measure the T_p, micellar size, zeta potential, and the rheology of polymer−surfactants complexes.

2. MATERIALS AND METHODS

2.1. Materials. Poly(ethylene oxide)−poly(propylene oxide)−poly(ethylene oxide) triblock copolymer F108 was purchased from Sigma. The average composition of PEO_{141}−PPO_{44}−PEO_{141} has a molar mass of 14 600 g mol^{-1}. Nonionic surfactant nonylphenol ethoxylate (NP9), cationic surfactant cetyltrimethylammonium bromide (CTAB), and anionic surfactant sodium dodecyl sulfate (SDS) were also purchased from Sigma. All chemicals were used without further purification. Stock solution of the copolymer and surfactant were prepared using milli-Q water with resistivity value of 18.2 mΩ cm. All samples were prepared and left to equilibrate for 48 h before measurements.

2.2. Methods. The size and zeta potential measurement were carried out at 25 °C by using dynamic light scattering (Malvern zeta nano sizer). It uses a 4 mW He−Ne laser operating at a wavelength of 633 nm and uses the noninvasive backscatter technology (173°). DLS exploits the Brownian motion of the suspended droplets to measure the size distribution of the particles. The electric field correlation function $g^{(1)}(t)$ can be written as the Laplace transform of the distribution of relaxation rates, $G(\Gamma)$: $g^{(1)}(t) = \int_0^\infty G(\Gamma) \exp(-\Gamma t) d\Gamma$, where Γ is the relaxation time, and t is the delay time. The exponential decay of the correlation of the intensity fluctuations originates from the Brownian motion of the micelles, which depends on the diffusivity of the micelles according to the equation $\Gamma = Dq^2$, where Γ is the relaxation or correlation constant, D is the effective translational diffusion coefficient, and q is the scattering vector. For optically isotropic rods, the normalized electric field correlation function could be fitted with a weighted sum of two or more exponential decays, where the first and second term corresponds to translational and the rotational diffusion about the center of mass of the rod, respectively.[30] From the diffusion coefficient (D), the hydrodynamic radius (R_H) of the solute particles can be calculated using the Stokes−Einstein equation $R_H = k_B T/6\pi\eta D$, where k_B is the Boltzmann constant, and η is the viscosity of the solvent. The zeta potential (ζ) is obtained from the electrophoretic mobility (u) using the Smoluchowsky equation $\xi = u\eta/\varepsilon$, where η and ε are the solution viscosity and the dielectric constant of the medium, respectively. The rheological measurements were carried out using a strain controlled rheometer from Anton Paar (MCR 301) with cone and plate geometry with a Peltier temperature controller system. The shear viscosity was measured at a constant shear rate of 10 s^{-1} in the temperature range 15−50 °C.

We have fixed the CMC of all three surfactants for a given concentration of F108 as it allows us to study the changes in the microstructure and elastic properties of block copolymers micelles for the same amount of surfactant micelles. Further, it is not practical to maintain the same ratio of relative amount of surfactant to F108 (e.g., 80 mM SDS/F108) in all three cases, as the amount of CTAB and NP9 required in those experiments would be very high (∼90 and 1250 CMC, respectively) that leads to local precipitation of surfactant in pluronic.

3. RESULTS AND DISCUSSION

3.1. Rheological Properties of Pluronics F108 with Surfactants. Figure 1a shows the viscosity as a function of temperature for 1, 4, 8, 10, 15, and 20 wt % of pluronics F108 at a constant shear rate of 10 s^{-1}. At low copolymer concentrations (1−4 wt %), the viscosity remains unchanged in the temperature range of 15 to 50 °C. At 4 wt %, a slight increase in viscosity is noticed at ∼30 °C, while at 8 wt %, viscosity increases drastically, above a temperature called the first percolation transition T_p, where the pluronics micelles start to form a permanent spanning structure. As the studied concentrations of F108 are above CMC (CMC for F108 is 0.7 wt %),[87] the aqueous solution contain micelles with a spherical core−shell geometry along with unimers. Above T_p, for higher concentrations, micelles can form highly ordered arrangements, where the coronae of neighboring micelles overlap. Under shear forces, the packing order is dominated by 2D hexagonally packed layers of micelles or a face-centered cubic (FCC) structure. Here, the self-assembly of micelles into layers, under shear forces, leads to the exceptional viscoelastic properties. The short-range attraction at elevated temperature, due to effective micellar interactions, is responsible for the observed dramatic increase in viscosity.[66,88] The T_p for 4, 8, 10 15, and 20 wt % of pluronics were 30, 28, 24, 20, and 13 °C,

dx.doi.org/10.1021/jp208902a | J. Phys. Chem. B 2012, 116, 1499−1507

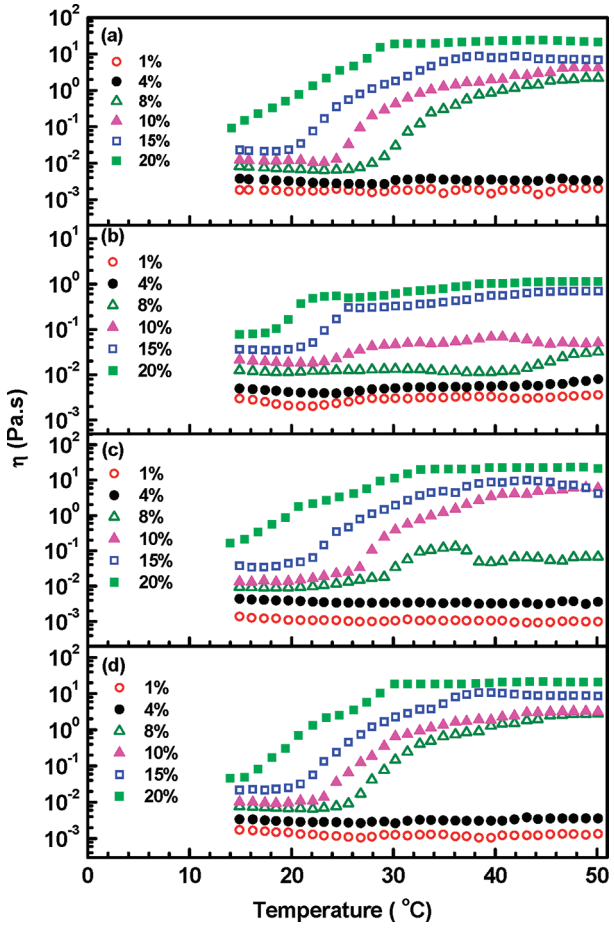

Figure 1. Viscosity as a function of temperature for pluronics F108 of different wt % (a) without surfactant and with (b) 10 CMC SDS, (c) 10 CMC CTAB, and (d) 10 CMC NP9. The measurements are performed at a constant shear rate of 10 s^{-1}.

respectively. As the studied concentrations of pluronics were relatively low, no structural arrest of micelles are observed at higher temperatures. The gel formation above percolation transition can be understood in terms of the formation of a permanent spanning structure that is seen in attractive colloidal systems.[89] The percolation transition occurs due to an additional intermicellar interaction and the excluded volume effect due to the finite size hard core.[21] The interpenetration of polymer chains and the consequent depletion of the solvent in the corona region occur when the intermicellar spacing is less than the diameter of the micelle.

Figure 1b shows the viscosity of copolymer F108 solution in the presence of 10 CMC SDS (i.e., 80 mM) as a function of temperature. At low copolymer concentrations, the viscosity remains constant in the temperature range 15−50 °C. This behavior is similar to that observed without surfactant. The average viscosity for 1 and 4 wt % of F108 with SDS, in the temperature range of 15−50 °C, is 2 and 4 mPa s, respectively. For 8 wt % of F108, the viscosity is constant in the temperature range of 15−42 °C, above which an increase in viscosity is observed. The onset of temperature at which the increase in viscosity occurs for 8, 10, 15, and 20 wt % of pluronics are 42, 23, 21, and 18 °C, respectively. The viscosity shows a plateau at higher temperature. Figure 1c shows the viscosity of pluronics F108 in the presence of 10 CMC CTAB (i.e., 9 mM) as a function of temperature. At low concentration of copolymer, the viscosity remains constant in the temperature range 15−50 °C, which is similar to that observed for pure copolymer solution. The average viscosity for 1 and 4 wt % of F108 with CTAB in the temperature range of 15−50 °C is 1.6 and 3.4 mPa s, respectively. The viscosity shows an abrupt increase above T_p when the copolymer wt % is increased from 8 to 20. The onset of increase in viscosity for 8, 10, 15, and 20 wt % of pluronics occurs at 28, 25, 20, and 12 °C, respectively. Figure 1d shows the viscosity of pluronics in the presence of 10 CMC NP9 (i.e., 0.64 mM) as a function of temperature. At low concentrations of copolymer, the viscosity remains constant in the temperature range of 15 to 50 °C. The average viscosity for 1 and 4 wt % of F108 with NP9 in the temperature range of 15 to 50 °C are 1.6 and 3.4 mPa s, respectively. However, at higher polymer concentrations, i.e., 8−20 wt %, viscosity increase is rapid. The T_p for 8, 10, 15, and 20 wt % of pluronics are 26, 23, 20, and 15 °C, respectively. The steady shear viscosity data in F108 shows a shear thinning behavior, which indicates that the 2D hexagonally close-packed layers of micelles form shear planes, which are arranged to minimize the resistance against laminar flow.[68] It has been found that there is a continuous transformation of unoriented domains into the shear-aligned orientation as the shear rate is increased. Analysis of the stacking sequence probabilities shows that the structure changes from asymmetrically twinned ABC (FCC) at low shear rates to a random AB stacking sequence at high shear rates.[68] The intralayer neighboring micelle center-to-center distances are found to be 20.5 and 19.2 nm for 20 and 30 wt % polymer solutions, respectively.

For spherical particles in simple shear flow, the Peclet number, $P_e = 6\pi\eta\dot{\gamma}a^3/kT$, where kT is the thermal energy (η the viscosity of the fluid, k being the Boltzmann's constant and T the absolute temperature),[90] characterizes the relative influence of shear flow to the diffusion caused by the thermal agitation, gives an idea about the hydrodynamic forces and Brownian drag present in the system. Thus, it determines the extent to which the microstructure is distorted away from the equilibrium by the flow field. Assuming a pluronic micellar size of 13 nm, the calculated value of P_e is $\sim(6.5 \times 10^{-5})$. Therefore, the $P_e \ll 1$ condition suggests that the thermal or Brownian motion overwhelms the imposed shear representing the thermodynamic equilibrium. Only under the condition of $P_e \gg 1$, the shearing motion can dominate.

Figure 2 shows the variation of T_p as a function of pluronics F108 concentration in the absence and presence of different surfactants. The concentration of each surfactants used is 10 times its CMC value. In all the cases, the T_p values decrease with increasing surfactant concentration. The results show that the T_p increases with SDS concentration and decays slowly with increasing ϕ. Generally, at a fixed ionic concentration, the aggregation number of copolymer in the mixed micelle increases with an increase in copolymer concentration where the micellar size and aggregation number is determined by copolymer concentration. The hydrophilic PEO in the corona portion of the mixed micelle increases, while the charge on the micellar interface decreases. The simultaneous decrease in charge and increase in temperature leads to a growth of micelles. The long-range repulsion and the reduced osmotic compressibility due to strong Coulombic interaction among the mixed micelles lead to a slow decay in T_p.[91] Also, in the presence of anionic SDS molecules, an increased hydration of the micelles is achieved due to the stretching of EO blocks in the corona region.[41] The decrease in T_p with increasing copolymer concentration can be due to weak entropic penalty.[20,92]

dx.doi.org/10.1021/jp208902a | J. Phys. Chem. B 2012, 116, 1499−1507

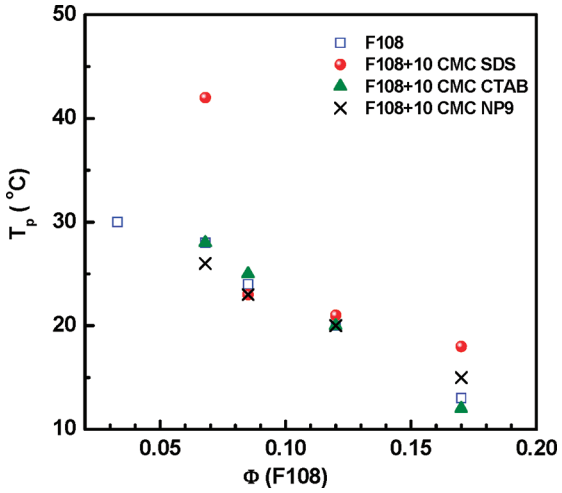

Figure 2. Percolation transition temperature (T_p) as a function of pluronics F108 volume fraction, without and with different surfactants of 10 CMC. The T_p is obtained from the viscosity enhancement at a shear rate of 10 s^{-1}.

It is known that the addition of SDS to triblock polymer solutions results in the adsorption of DS^- chains to the hydrophobic central PPO core of the triblock micelles. This imparts negative charges to the mixed aggregates, and the intra-aggregate repulsion leads to the breakdown of large spherical micelles into smaller mixed micelles comprising of both triblock and SDS.[93,94] At low F108 concentrations (1–4 wt %), the surfactant micelles prevent the self-assembly of F108 micelles due to effective electrostatic repulsion. This was evident from the flat viscosity profile with temperature at lower polymer concentrations. However, at higher copolymer concentrations (8–15 wt %), the electrostatic repulsion among the surfactant headgroup reduces due to the penetration of hydrophilic PEO that favors micellar assembly and growth. Therefore, the addition of small amounts of SDS can result in the formation of large copolymer-rich charged complexes, while larger amount of SDS results in the breakup of these complexes and the formation of smaller surfactant-rich complexes.

Comparison of the viscosity of pure F108 (8 wt %) and the one with 10 CMC of CTAB shows that the viscosity increase is an order of magnitude lower in the latter case at 40 °C. It has been found that the addition of CTAB to the copolymer micellar solution forms a supramolecular assembly where the hydrophobic long chain of the CTAB molecule gets dissolved in the core of copolymer micelle.[84] The charged headgroup of CTAB molecules resides at the interface of core and corona of the micelle and the charge density of the layer in the copolymer micelle decreases gradually with an increase in copolymer concentration. The constant viscosity observed at low polymer concentration indicates the absence of micellar self-assembly. In mixed NP9–F108 solution, the transition temperature decreases from 26 to 20 °C as the concentration of copolymer is increased. A study on the mixed micelle formation of aqueous P123 triblock copolymer with $C_{12}EO_6$ nonionic surfactant shows that the size of mixed micelles depends on the amount of $C_{12}EO_6$ and temperature.[53]

Figure 3 shows the elastic (G') and loss (G'') moduli as a function of angular frequency for pure pluronics F108 of 15 wt % and with SDS, CTAB, and NP9. The surfactant concentrations in all three cases are 10 times the CMC, and the sample temperature is 40 °C. The applied oscillatory strain amplitude is 0.5%.

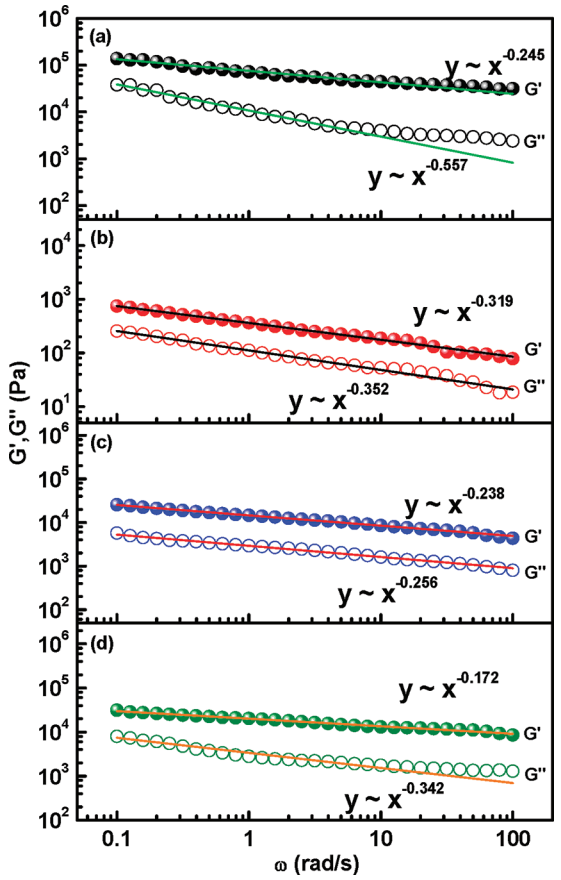

Figure 3. Viscoelastic moduli as a function of angular frequency for pluronics F108 15 wt % (a) without surfactant, (b) with SDS, (c) with CTAB, and (d) with NP9. The sample temperature is 40 °C in all the cases, and the surfactant concentration is 10 times the CMC value of surfactants.

The important observations from Figure 3 are that (1) the elastic modulus G' is greater than the viscous modulus G'', which indicates the elastic behavior of the material and that (2) the moduli are both weakly dependent on frequency indicating the structural changes in the system. The average G' value for 15 wt % F108 with 10 CMC of SDS and without SDS are ~10^3 and 10^5 Pa, respectively. The 2 orders of magnitude decrease in the elastic modulus in the presence of SDS indicates the dramatic reduction in the mechanical properties of the pluronics self-assembled network structures upon the addition of SDS. This corroborates the fact that the strong electrostatic barriers imparted by the micellar interface by SDS molecules at the core–corona interface restrict the self-assembly and the growth of micelles.

Both G' and G'' show a power law decay ($\omega^{-\upsilon}$), with frequency (ω) and the decay exponent values (υ) as indicated in Figure 3. The G' and G'' decay faster when SDS is present in the pluronic. This indicates that the elastic structure formed by F108 with anionic surfactants is softer than pure F108 and with CTAB and NP9. The decrease in the elastic modulus of samples with anionic surfactants again support the earlier finding that the charged layer at the interface of the core–corona region restricts the self-assembling of micelles. As the surface charge density of SDS (~0.606 C/m^2)[95] is much higher compared to that of CTAB (~0.362 C/m^2), the effect was more dominant in the case of SDS. Force measurements between polymer covered emulsion droplets in the presence of SDS and CTAB show a dramatic enhancement in the onset of repulsion in the former case, which

dx.doi.org/10.1021/jp208902a | J. Phys. Chem. B 2012, 116, 1499–1507

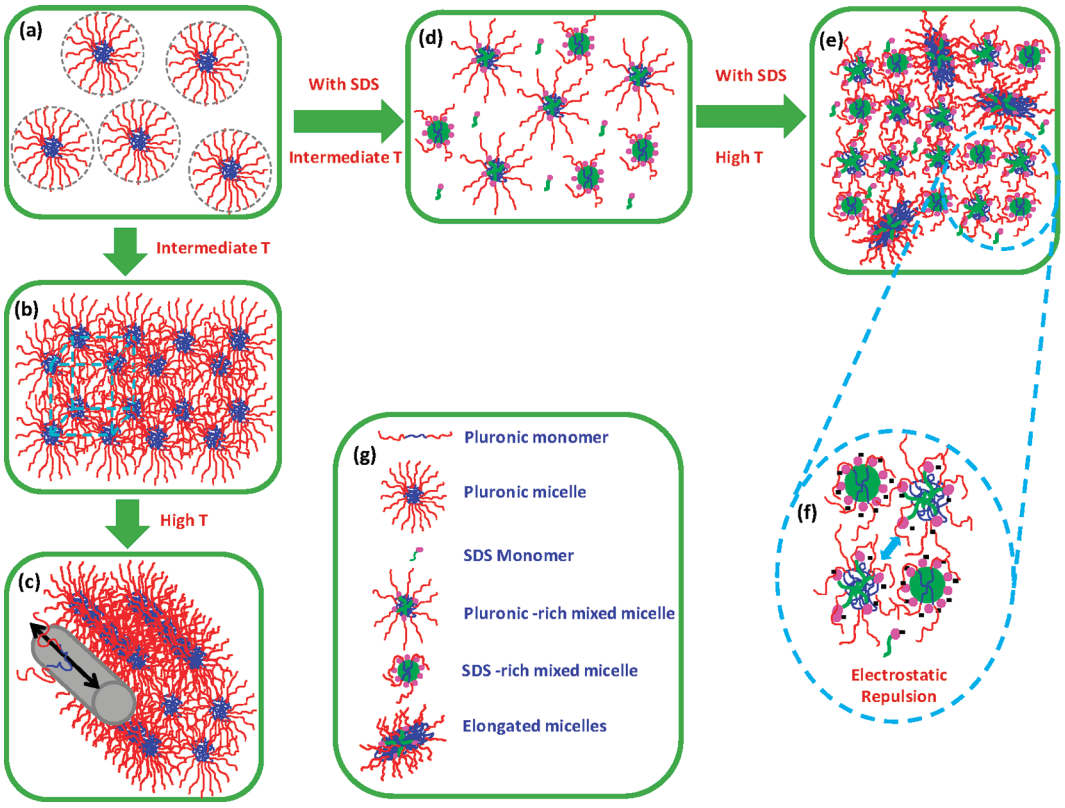

Figure 4. Schematics showing the micellar aggregates of pure pluronic F108 and with addition of surfactant; (a) pure pluronics at low temperature showing micellar aggregates, (b) pure pluronics at intermediate temperature, (c) pure pluronics F108 at high temperature, (d) pluronics with SDS at intermediate temperature, (e) pluronics with SDS at high temperature, and (f) magnified view of the intermicellar clusters exhibiting electrostatic repulsion.

was attributed to stretching of the tail regions of the polymers due to strong repulsion between head groups.[96] The expected nature of the micellar conformation of pluronic in the absence and presence of anionic surfactant head groups is depicted in the cartoon of Figure 4.

Figure 5 shows the viscosity of pluronics F108 (15 wt %) for different concentrations of SDS at a shear rate of 10 s^{-1} in the temperature range of 15 to 50 °C. At 5 CMC of SDS (i.e., 40 mM), the onset of the increase in viscosity is observed at 26 °C, which is slightly higher than that of pure copolymer. However, the viscosity at 40 °C is lower than that of the pure copolymer. At 10 CMC SDS, the T_p remains the same, but the plateau viscosity is reduced by more than an order of magnitude. With further increase in SDS (15 CMC), the transition temperature is almost continuous, and the plateau viscosity is reduced by more than 2 orders of magnitude. The photograph of pure F108 (15 wt %) and F108 (15 wt %) with 10 CMC SDS is shown in Figure 6. The former shows a strong viscoelastic behavior, and the sample holds its weight when inverted, while the latter shows liquid like behavior.

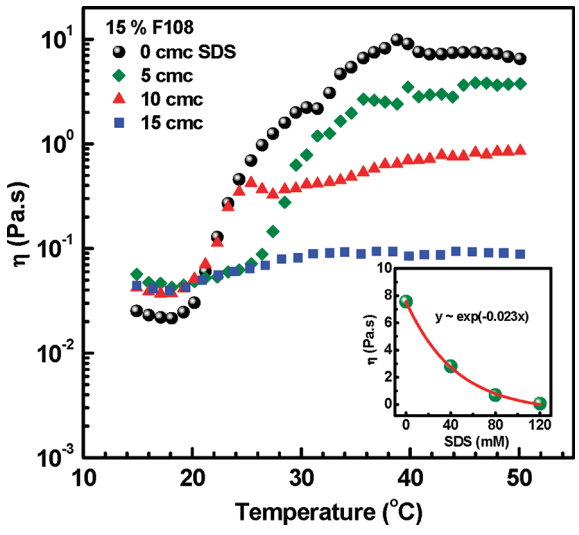

Figure 5. Viscosity as a function of temperature of 15 wt % of pluronics F108 with different concentration of SDS at a shear rate of 10 s^{-1}. The inset shows the viscosity value of 15 wt % F108 at different concentration of SDS at 40 °C. The bold line is an exponential fit to the data points.

As the SDS concentration increases from 0 to 15 CMC, the plateau regime of the viscosity curve is progressively decreased. Overall, the viscosity at higher temperature follows an exponential decay with SDS concentration where the decay constant is found to be 0.023 (Figure 5, inset). The addition of SDS to F108 solutions results in the adsorption of the dodecyl sulfate ion (DS^-) chains to the hydrophobic central PPO core of the F108 micelles. This imparts negative charges to these mixed aggregates, and the intra-aggregate repulsion leads to the breakdown of the large spherical micelles into smaller mixed micelles comprising both F108 and SDS.[93,94] In the case of 5 CMC SDS, the sample contains a large amount of copolymer rich mixed micelles, and hence the growth is favorable due to entropic conditions. Further addition of surfactant leads to degradation of copolymer−rich micelles and an increase in the number density of SDS rich micelles. This explains the

dx.doi.org/10.1021/jp208902a | J. Phys. Chem. B 2012, 116, 1499−1507

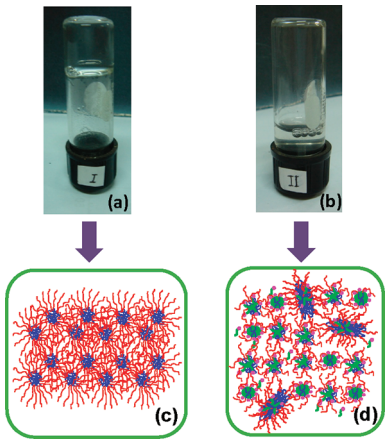

Figure 6. Photographs of (a) 15 wt % F108 alone where the sample is gel-like holding its weight on the inverted vial; (b) 15 wt % F108 + 10 CMC SDS where the sample exhibits fluid-like behavior; (c, d) schematic representation of pluronic micelles in panels a and b. The sample temperature was 40 °C.

observed decrease in viscosity by an order of magnitude. The addition of excess surfactants (15 CMC) leads to a complete degradation of the pure copolymer micelles where the system is dominated by a mixture of SDS-rich micelles and pure SDS micelles. Further, the presence of charged species at higher CMC enhances the fluidity of the sample due to intermicellar repulsion that makes the condition unfavorable for growth of micelles and a reduction in viscosity. These results show that the rheology of the block copolymer can be tuned by varying the concentrations of ionic surfactant. Further, the T_p is shifted to lower temperature as the SDS concentration increases.

Figure 7 shows the frequency sweep for 15 wt % pluronics at different concentrations of SDS at 40 °C. For all the

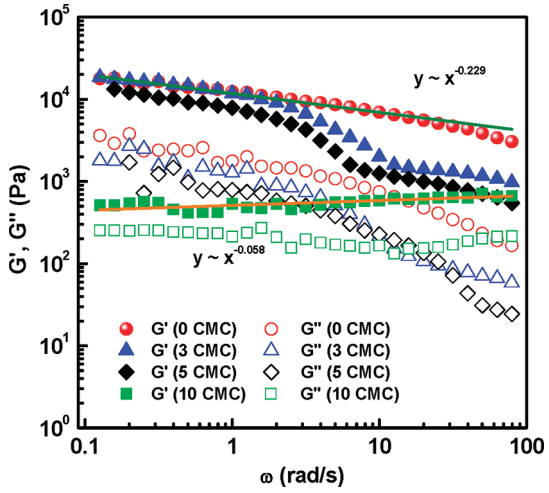

Figure 7. Elastic (G') and storage (G'') moduli as a function of angular frequency for 15 wt % F108 at different SDS concentration performed at 40 °C.

SDS concentrations, $G' > G''$ indicates that elastic properties dominate over the viscous properties at higher temperatures. At 0 CMC, both G' and G'' show a weak dependence on frequency where G' is an order of magnitude larger than G''. For three and five times CMC of SDS, a sudden decrease in the G' is observed at 6 rad/s indicating the weakening of the microstructure due to internal deformation. In the above three cases, the G'' show a relatively strong dependence on frequency. At 10 CMC of SDS, both G' and G'' becomes frequency independent, and their magnitude drops drastically indicating the good mechanical stability of the soft structure formed. Even at 10 CMC of SDS, G' prevails over G'' indicating the elastic nature of the microstructure.

3.2. Size and Zeta Potential Measurement. Figure 8a shows the size distribution of F108 micelles (1 wt %) at

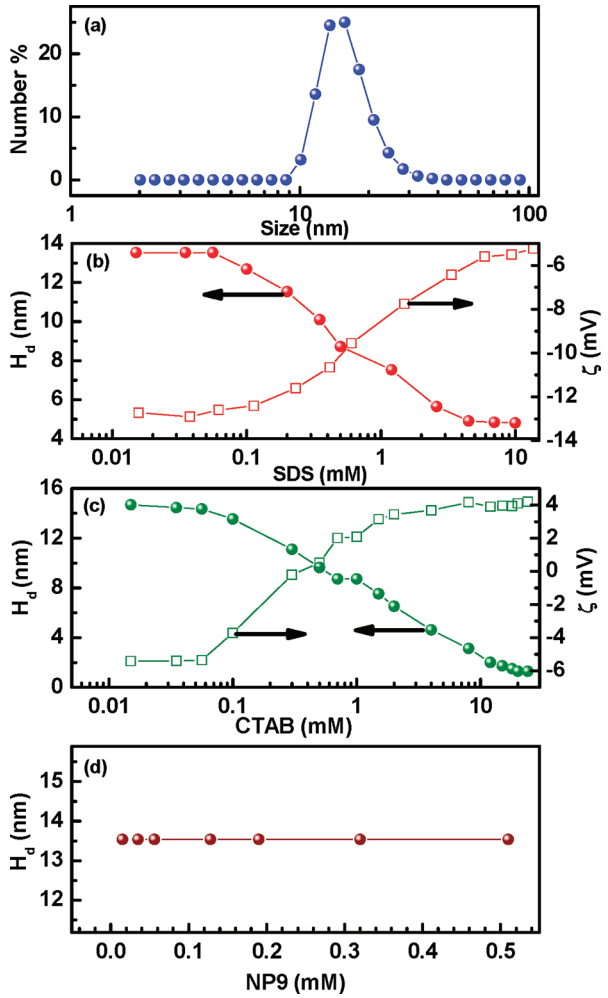

Figure 8. (a) Size distribution of 1 wt % pluronics F108, (b) ζ potential of 1 wt % F108 at varying SDS, and (c) ζ potential of 1 wt % F108 at varying CTAB; measurements performed at 40 °C.

40 °C. The hydrodynamic diameter (H_d) of pure pluronics F108 at 40 °C is found to be ~14 nm. Figure 8b shows the variation of H_d and the zeta potential (ζ) of 1 wt % pluronics F108 as a function of SDS concentration. The temperature at which these measurements were made is 40 °C. For 1 wt % pluronics F108, the H_d value remains constant at ~14 nm in the SDS concentration range of 0.01 to 0.06 mM. In the SDS concentration range of 0.06 to 4 mM, the H_d decreases from 14 to 5 nm. Beyond 4 mM SDS, the H_d remains constant.

The ζ remains constant at ~−13.5 mV for the SDS concentration of 0.01 to 0.06 mM. Above 0.06 mM, the ζ value decreases from −13.5 to −7 mV up to the SDS concentration of 4 mM. Beyond 4 mM, the ζ remains constant. Similar weakly negative zeta potentials (−3 to −7 mV) are

dx.doi.org/10.1021/jp208902a | J. Phys. Chem. B 2012, 116, 1499–1507

observed for the PDEA−core micelle of poly(ethylene oxide-block-2-(diethylamino)ethyl methacrylate) (PEO−PDEA) above pH 8.5.[97] The morphological changes caused by alteration in the local Coulombic interactions within the nanostructures is evident in the ζ measurements. As the ζ is a measure of the electric field potential at the micelle's plane of zero shear, it is affected by the size, shape, and surface charge of the structure. The reduction in the ζ values with increasing surfactant concentration also indicates a reduction in the surface area (size) of the pluronics mixed micelles.

Figure 8c shows the size and zeta potential of 1 wt % F108 as a function of CTAB concentration. The zeta potential value was ∼−5 mV in the CTAB concentration range from 0.01 to 0.04 mM. Above 0.04 mM, the zeta potential value changes from −5.6 mV to +4 mV up to the CTAB concentration of 10 mM. Beyond 10 mM, the zeta potential remains constant. The H_d value remains constant at 14 nm in the CTAB concentration range 0.01 to 0.04 mM. As the CTAB concentration increases from 0.04 mM to 15 mM, the H_d decreases from 14 to 1.9 nm. Beyond 15 mM, the H_d remains at 1.9 nm, which corresponds to the size of pure CTAB micelles. Figure 8d shows the size of 1 wt % F108 as a function of NP9 concentration where no change in the size of pluronics micelles is observed.

Figure 9a−c shows the normalized autocorrelation coefficient as a function of delay time for 1 wt % F108 with SDS, CTAB, and NP9, respectively. The measurements were made at 40 °C. As the surfactant concentration increases, the autocorrelation function changes from single exponential form (i.e., $\exp(-t/\tau)$) to a stretched multiexponential form,[98] e.g., biexponential form of $g^1(t) = A_f \exp(-t/\tau_f) + A_s \exp[(-t/\tau_s)^\beta])$, where A_f and A_s are the amplitudes for the fast and slow relaxation modes corresponding to the relaxation time τ_f and τ_s, respectively, and β is the stretching exponent.[99] Here, τ is the relaxation time, which is related to the translational diffusion coefficient as $1/\tau = Dq^2$, where $q = (4\pi n/\lambda)\sin(\theta/2)$. Figure 9a data for 0.05 mM SDS is well represented by a single exponential decay curve where the calculated diffusion coefficient is found to be 6.51×10^{-11} m^2 s^{-1}, and the corresponding H_d value is 8.82 nm. For 8.1 mM SDS, the data points are fitted with a bimodal decay curve where the diffusion coefficients are 2.92×10^{-10} m^2 s^{-1} and 4.5×10^{-11} m^2 s^{-1}, and the corresponding H_d values are 1.96 and 12.73 nm, respectively. A similar trend in the autocorrelation function is observed for CTAB. The calculated diffusion coefficient at a CTAB concentration of 0.02 mM is 6.01×10^{-11} m^2 s^{-1}, and the corresponding H_d value is 9.53 nm. For 12.1 mM CTAB, the bimodal decay fit gave two diffusion coefficients 2.49×10^{-10} and 4.1×10^{-12} m^2 s^{-1}, and the corresponding H_d values are 2.3 and 139 nm, respectively. However, for NP9, the correlogram remains the same irrespective of the quantity of NP9. The diffusion coefficient obtained from the fit is found to be 5.18×10^{-11} m^2 s^{-1}, corresponding to an average H_d value of 11.07 nm. The DLS studies in nongelling aqueous solutions of pluronic F68 show the existence of two relaxation modes (a single exponential at short time and a stretched exponential tail at long times) and a power law depending on the temperature and concentration.[98] Because of the higher headgroup charge of the ionic surfactant and the screening of the hydrophobic parts of the polymer, the aggregates become highly hydrophilic and remain as monomers rather than forming micelles. This explains the decrease in H_d of the F108−SDS system at high ionic surfactant concentrations.

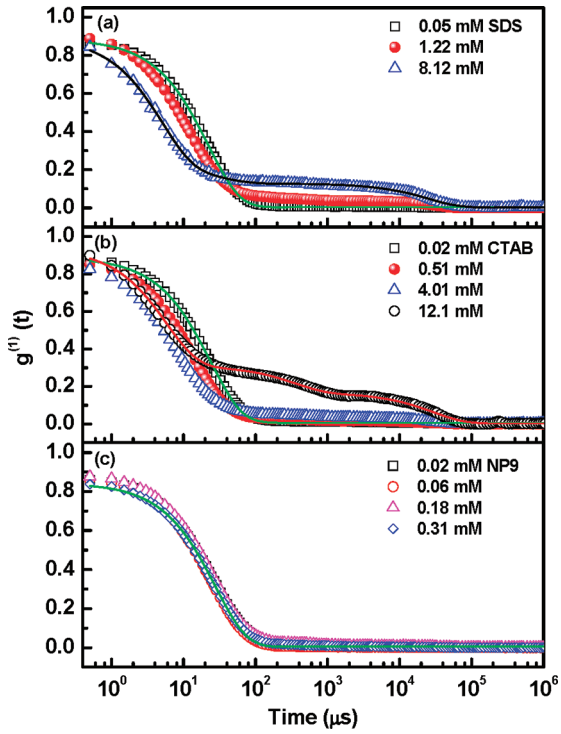

Figure 9. Normalized autocorrelation function versus delay time for 1 wt % F108 with (a) SDS, (b) CTAB, and (c) NP9 at 40 °C.

Our experimental results on H_d, zeta potential, and viscosity suggest three possibilities. At low surfactant concentrations, monomeric surfactant molecules associate with the polymer micelles with a large copolymer-rich complex that are highly charged. At the intermediate surfactant concentrations, copolymer−surfactant complexes coexist. The polymer complexes are progressively disintegrated with increasing surfactant concentration. At high surfactant concentrations, only small surfactant-rich complexes are present. The large changes in the H_d and zeta potential in presence of surfactant in micellized triblock copolymer show the strong interaction between them and the resulting changes in the physicochemical parameters. These observations are consistent with earlier studies.[82,84,100,101]

4. CONCLUSIONS

We studied the interaction of a triblock copolymer F108 with ionic and nonionic surfactants and its influence on percolation transition temperature T_p, rheology, size, and zeta potential. T_p is found to decrease with volume fraction of surfactants, irrespective of the nature of surfactant used. The decrease in T_p with volume fraction of the triblock polymer−SDS mixed system is much slower compared to pure, cationic, and nonionic cases. The rheological studies show that the viscosity changes with temperature was dramatic with SDS compared to CTAB and NP9. The important observations from the rheological results are that (1) the elastic modulus G' is greater than the viscous modulus G'' indicating the elastic behavior of the material and that (2) both the moduli are weakly dependent on frequency. The average G' value for 15 wt % F108 with 10 CMC of SDS and without SDS are ∼10^3 and 10^5 Pa, respectively. The 2 orders of magnitude decrease in the elastic modulus in the presence of SDS indicates the dramatic reduction in the mechanical properties of the self-assembled network structures of pluronics upon the addition of SDS, which corroborates the fact that the strong

dx.doi.org/10.1021/jp208902a | J. Phys. Chem. B 2012, 116, 1499−1507

electrostatic barriers imparted by the micellar interface by SDS molecules at the core−corona interface restrict the self-assembly and the growth of micelles. The hydrodynamic diameter of F108−SDS mixed micelle at 40 °C decreases from ∼14 to 5 nm, as SDS concentration increases from 0.06 to 4 mM.

AUTHOR INFORMATION

Corresponding Author

*Phone: 00-91-9443151536. Fax: 91-44-27480356. E-mail: philip@igcar.gov.in.

ACKNOWLEDGMENTS

J.P. thanks Mr. S. C. Chetal, Director, IGCAR, and Dr. T. Jayakumar, Director, Metallurgy and Materials Group, for supporting the advanced nanofluid program and fruitful discussions. J.P. also thanks BRNS for funding of a perspective research grant on the development of advanced nanofluids for diverse applications.

REFERENCES

(1) Lindman, B.; Thalberg, K.; Goodard, E. D.; Ananthapadmanabhan, K. P., Eds. *Interactions of Surfactants with Polymers and Proteins*; CRC Press: Boca Raton, FL, 1993.

(2) Hamley, I. W. *Block Copolymers in Solution*; Wiley, Chichester, U.K., 2005.

(3) Alexandridis, P.; Holzwarth, J. F.; Hatton, T. A. *Macromolecules* **1994**, *27*, 2414−2425.

(4) Nakashima, K.; Bahadur, P. *J. Controlled Release* **2002**, *82*, 189.

(5) Krishnamoorthy, S.; Pugin, R.; Brugger, J.; Heinzelmann, H.; Hoogerwerf, A. C.; Hinderling, C. *Langmuir* **2006**, *22*, 3450.

(6) Sakai, T.; Alexandridis, P. *Nanotechnology* **2005**, *16*, S344.

(7) Lin, Y.; Daga, V. K.; Anderson, E. R.; Gido, S. P.; Watkins, J. J. *J. Am. Chem. Soc.* **2011**, *133*, 6513−6516.

(8) Alexander, S.; Cosgrove, T.; Prescott, S. W.; Castle, T. C. *Langmuir* **2011**, *27*, 8054−8060.

(9) Liu, S.; Weaver, J. V. M.; Tang, Y.; Billingham, N. C.; Armes, S. P. *Macromolecules* **2002**, No. 35, 6121−6131.

(10) Mohan, P. H.; Bandyopadhyay, R. *Phys. Rev. E* **2008**, *77*, 041803.

(11) Wang, Q.; Li, L.; Jiang, S. *Langmuir* **2005**, *21*, 9068−9075.

(12) Vieira, J. B.; Thomas, R. K.; Li, Z. X.; Penfold, J. *Langmuir* **2005**, *21*, 4441−4451.

(13) Mata, J. P.; Majhi, P. R.; Guo, C.; Liu, H. Z.; Bahadur, P. *J. Colloid Interface Sci.* **2005**, *292*, 548−556.

(14) Tang, P.; Qiu, F.; Zhang, H.; Yang, Y. *Phys. Rev. E* **2004**, *69*, 031803.

(15) Lindner, H.; Scherf, G.; Glatter, O. *Phys. Rev. E* **2003**, *67*, 061402.

(16) Inomata, K.; Nakanishi, D.; Banno, A.; Nakanishi, E.; Abe, Y.; Kurihara, R.; Fujimoto, K.; Nose, T. *Polymer* **2003**, *44*, 5303−5310.

(17) Thurn, T.; Couderc, S.; Sidhu, J.; Bloor, D. M.; Penfold, J.; Holzwarth, J. F.; Jones, E. W. *Langmuir* **2002**, *18*, 9267−9275.

(18) Senkow, S.; Mehta, S. K.; Douheret, G.; Roux, A. H.; Desgranges, G. R. *Phys. Chem. Chem. Phys.* **2002**, *4*, 4472−4480.

(19) Banaszak, M.; Wołoszczuk, S.; Pakula, T.; Jurga, S. *Phys. Rev. E* **2002**, *66*, 031804.

(20) Michels, B.; Waton, G.; Zana, R. *Colloids Surf. A* **2001**, *183*, 55−65.

(21) Lobry, L.; Micali, N.; Mallamace, F.; Liao, C.; Chen, S. H. *Phys. Rev. E* **1999**, *60*, 7076−7087.

(22) Neumann, C.; Abetz, V.; Stadler, R. *Colloid Polym. Sci.* **1998**, *276*, 19−27.

(23) Liu, Y.; Chen, S. H.; Huang, J. S. *Macromolecules* **1998**, *31*, 2236−2244.

(24) Caragheorgheopol, A.; Schlick, S. *Macromolecules* **1998**, *31*, 7736−7745.

(25) Yu, J. M.; Jerome, R.; Teyssie, P. *Polymer* **1997**, *38*, 347−354.

(26) Wu, C.; Liu, T.; Chu, B.; Schneider, D. K.; Graziano, V. *Macromolecules* **1997**, *30*, 4574−4583.

(27) Mortensen, K. *J. Phys.: Condens. Matter* **1996**, *8*, A103−A124.

(28) Zhou, Z.; Chu, B. *Macromolecules* **1994**, *27*, 2025−2033.

(29) Wanka, G.; Hoffmann, H.; Ulbricht, W. *Macromolecules* **1994**, *27*, 4145−4159.

(30) Schillen, K.; Brown, W.; Johnsen, R. M. *Macromolecules* **1994**, *27*, 4825−4832.

(31) Hvidt, S.; Joergensen, E. B.; Brown, W.; Schillen, K. *J. Phys. Chem.* **1994**, *98*, 12320−12328.

(32) Mortensen, K.; Pedersen, J. S. *Macromolecules* **1993**, *26*, 805−812.

(33) Mortensen, K.; Brown, W. *Macromolecules* **1993**, *26*, 4128−4135.

(34) Brown, W.; Schillen, K.; Hvidt, S. *J. Phys. Chem.* **1992**, *96*, 6038−6044.

(35) Brown, W.; Schillen, K.; Almgren, M.; Hvidt, S.; Bahadur, P. *J. Phys. Chem.* **1991**, *95*, 1850−1858.

(36) Chen, W. R.; Chen, S. H.; Mallamace, F. *Phys. Rev. E* **2002**, *66*, 021403.

(37) Zheng, L.; Guo, C.; Wang, J.; Liang, X.; Chen, S.; Ma, J.; Yang, B.; Jiang, Y.; Liu, H. *J. Phys. Chem. B* **2007**, *111*, 1327−1333.

(38) Weiss, J.; Laschewsky, A. *Langmuir* **2011**, *27*, 4465−4473.

(39) Jiang, T.; Wang, L.; Lin, S.; Lin, J.; Li, Y. *Langmuir* **2011**, *27*, 6440−6448.

(40) Ulrich, K.; Galvosas, P.; Karger, J.; Grinberg, F. *Phys. Rev. Lett.* **2009**, *102*, 037801.

(41) Ganguly, R.; Aswal, V. K.; Hassan, P. A.; Gopalakrishnan, I. K.; Kulshreshtha, S. K. *J. Phys. Chem. B* **2006**, *110*, 9843−9849.

(42) Maniadis, P.; Thompson, R. B.; Rasmussen, K. O.; Lookman, T. *Phys. Rev. E* **2004**, *69*, 031801.

(43) Hamley, I. W. *J. Phys.: Condens. Matter* **2001**, *13*, R643−R671.

(44) Tanner, S. A.; Amin, S.; Kloxin, C. J.; Zanten, J. H. V. *J. Chem. Phys.* **2011**, *134*, 174903.

(45) O'Lenick, T. G.; Jin, N.; Woodcock, J. W.; Zhao, B. *J. Phys. Chem. B* **2011**, *115*, 2870−2881.

(46) Bossard, F.; Sfika, V.; Tsitsilianis, C. *Macromolecules* **2004**, *37*, 3899−3904.

(47) Slawecki, T. M.; Glinka, C. J.; Hammouda, B. *Phys. Rev. E* **1998**, *58*, R4084−R4087.

(48) Newby, G. E.; Hamley, I. W.; King, S. M.; Martin, C. M.; Terrill, N. J. *J. Colloid Interface Sci.* **2009**, *329*, 54−61.

(49) Deyerle, B. A.; Zhang, Y. *Langmuir* **2011**, *27*, 9203−9210.

(50) Li, Y.; Bao, M.; Wang, Z.; Zhang, H.; Xu, G. *J. Mol. Struct.* **2011**, *985*, 391−396.

(51) Mahajan, R. K.; Shaheen, A.; Sachar, S. *J. Dispersion Sci. Technol.* **2009**, *30*, 1020−1026.

(52) Lof, D.; Tomsic, M.; Glatter, O.; Popovski, G. F.; Schillen, K. *J. Phys. Chem. B* **2009**, *113*, 5478−5486.

(53) Schillen, K.; Jansson, J.; Lof, D.; Costa, T. *J. Phys. Chem. B* **2008**, *112*, 5551−5562.

(54) Lof, D.; Niemiec, A.; Schillen, K.; Loh, W.; Olofsson, G. *J. Phys. Chem. B* **2007**, *111*, 5911−5920.

(55) Barbosa, S.; Taboada, P.; Castro, E.; Mosquera, V. *J. Colloid Interface Sci.* **2006**, *296*, 677−684.

(56) Jansson, J.; Schillen, K.; Nilsson, M.; Soderman, O.; Fritz, G.; Bergmann, A.; Glatter, O. *J. Phys. Chem. B* **2005**, *109*, 7073−7083.

(57) Jansson, J.; Schillen, K.; Olofsson, G.; Silva, R. C. D.; Loh, W. *J. Phys. Chem. B* **2004**, *108*, 82−92.

(58) Almgren, M.; Stam, J. V.; Lindblad, C.; Li, P.; Stilbs, P.; Bahadur, P. *J. Phys. Chem.* **1991**, *95*, 5677−5684.

(59) Sun, K.; Kumar, R.; Falvey, D. E.; Raghavan, S. R. *J. Am. Chem. Soc.* **2009**, *131*, 7135−7141.

(60) Kjoniksen, A.-L.; Zhu, K.; Behrens, M. A.; Pedersen, J. S.; Nystrm, B. *J. Phys. Chem. B* **2011**, *115*, 2125−2139.

(61) Huff, A.; Patton, K.; Odhner, H.; Jacobs, D. T.; Clover, B. C.; Greer, S. C. *Langmuir* **2011**, *27*, 1707−1712.

(62) Yang, L.; Guo, C.; Jia, L.; Xie, K.; Shou, Q.; Liu, H. *Ind. Eng. Chem. Res.* **2010**, *49*, 8518−8525.

(63) Hamley, I. W. *Curr. Opin. Colloid Interface Sci.* **2000**, *5*, 342−350.
(64) Chu, B. *Langmuir* **1995**, *11*, 414−421.
(65) Michels, B.; Waton, G.; Zana, R. *Colloids Surf. A* **2001**, *183*, 55.
(66) Duval, M.; Waton, G.; Schosseler, F. *Langmuir* **2005**, *21*, 4904−4911.
(67) Aswal, V. K.; Goyal, P. S.; Kohlbrecher, J.; Bahadur, P. *Chem. Phys. Lett.* **2001**, *349*, 458−462.
(68) Jiang, J.; Burger, C.; Li, C.; Li, J.; Lin, M. Y.; Colby, R. H.; Rafailovich, M. H.; Sokolov, J. C. *Macromolecules* **2007**, *40*, 4016−4022.
(69) Bahadur, P.; Pandya, K. *Langmuir* **1992**, *8*, 2666−2670.
(70) Linse, P.; Malmsten, M. *Macromolecules* **1992**, *25*, 5434−5439.
(71) Borbely, S. *Phys. B* **1998**, *241−243*, 1016−1018.
(72) Bohorquez, M.; Koch, C.; Trygstad, T.; Pandit, N. *J. Colloid Interface Sci.* **1999**, *216*, 34−40.
(73) Yang, L.; Alexandridis, P.; Steytler, D. C.; Kositza, M. J.; Holzwarth, J. F. *Langmuir* **2000**, *16*, 8555−8561.
(74) Trong, L. C. P.; Djabourov, M.; Ponton, A. *J. Colloid Interface Sci.* **2008**, *328*, 278−287.
(75) Chu, B.; Zhou, Z.; Nace, V. M. Physical Chemistry of Polyoxyalkylene Block Copolymer Surfactants. In *Nonionic Surfactants*; Marcel Dekker: New York, 1996; Vol. *60*.
(76) Nakashima, K.; Bahadur, P. *Adv. Colloid Interface Sci.* **2006**, *123*, 75−96.
(77) Alexandridis, P.; Hatton, T. A. *Colloids Surf. A* **1995**, *96*, 1−46.
(78) Jorgensen, E. B.; Hvidt, S.; Brown, W.; Schillen, K. *Macromolecules* **1997**, *30*, 2355−2364.
(79) Guo, L.; Colby, R. H.; Thiyagarajan, P. *Phys. B* **2006**, *385*, 685−687.
(80) Philip, J.; Prakash, G. G.; Jaykumar, T.; Kalynasundaram, P.; Mondain Monval, O.; Raj, B. *Langmuir* **2002**, *18*, 4625−4631.
(81) Jonsson, B.; Lindman, B.; Holmberg, K.; Kronberg, B. *Surfactants and Polymers in Aqueous Solution*; John Wiley & Sons: Chichester, U.K, 1998.
(82) Hecht, E.; Mortensen, K.; Gradzielski, M.; Hoffmann, H. *J. Phys. Chem.* **1995**, *99*, 4866−4874.
(83) Li, Y.; Xu, R.; Couderc, S.; Bloor, D. M.; Holzwarth, J. F.; Jones, E. W. *Langmuir* **2001**, *17*, 5742−5747.
(84) Singh, P. K.; Kumbhakar, M.; Ganguly, R.; Aswal, V. K.; Pal, H.; Nath, S. *J. Phys. Chem. B* **2010**, *114*, 3818−3826.
(85) Youssry, M.; Asaro, F.; Coppola, L.; Gentile, L.; Nicotera, I. *J. Colloid Interface Sci.* **2010**, *342*, 348−353.
(86) Couderc, S.; Li, Y.; Bloor, D. M.; Holzwarth, J. F.; Jones, E. W. *Langmuir* **2001**, *17*, 4818−4824.
(87) Lopes, J. R.; Loh, W. *Langmuir* **1998**, *14*, 750−756.
(88) Waton, G.; Michels, B.; Steyer, A.; Schosseler, F. *Macromolecules* **2004**, *37*, 2313−2321.
(89) Mallamace, F.; Chen, S. H.; Coniglio, A.; Arcangelis, L. D.; Gado, E. D.; Fierro, A. *Phys. Rev. E* **2006**, *73*, 020402.
(90) Melrose, J. R.; van Vliet, J. H.; Ball, R. C. *Phys. Rev. Lett.* **1996**, *77*, 4660.
(91) Nettesheim, F.; Zipfel, J.; Lindner, P.; Richtering, W. *Colloids Surf. A* **2001**, *183*, 563−574.
(92) Su, Y. L.; Liu, H. Z.; Wang, J.; Chen, J. Y. *Langmuir* **2002**, *18*, 865−871.
(93) Hecht, E.; Hoffmann, H. *Langmuir* **1994**, *10*, 86−91.
(94) Sastry, N. V.; Hoffmann, H. *Colloids Surf. A* **2004**, *250*, 247−261.
(95) Luo, G.; Wang, H. *J. Dispersion Sci. Technol.* **2007**, *28*, 1108−1111.
(96) Philip, J.; Gnanaprakash, G.; Jayakumar, T.; Kalyanasundaram, P.; Raj, B. *Macromolecules* **2003**, *36*, 9230−9236.
(97) Weaver, J. V. M; Armes, S. P.; Liu, S. *Macromolecules* **2003**, *36*, 9994−9998.
(98) Nystrom, B.; Kjoniksen, A. L. *Langmuir* **1997**, *13*, 4520−4526.
(99) Kadam, Y.; Ganguly, R.; Kumbhakar, M.; Aswal, V. K.; Hassan, P. A.; Bahadur, P. *J. Phys. Chem. B* **2009**, *113*, 16296−16302.
(100) Li, Y.; Xu, R.; Bloor, D. M.; Holzwarth, J. F.; Jones, E. W. *Langmuir* **2000**, *16*, 10515−10520.
(101) Li, Y.; Xu, R.; Couderc, S.; Bloor, D. M.; Jones, E. W.; Holzwarth, J. F. *Langmuir* **2001**, *17*, 183−188.